ACS APPLIED MATERIALS & INTERFACES

Research Article

Cite This: ACS Appl. Mater. Interfaces 2019, 11, 22777−22785

www.acsami.org

Large-Area and Water Rewriteable Photonic Crystal Films Obtained by the Thermal Assisted Air−Liquid Interface Self Assembly

Shuzhen Yu, Xu Cao, Wenbin Niu, Suli Wu, Wei Ma, and Shufen Zhang*

State Key Laboratory of Fine Chemicals, Dalian University of Technology, West Campus, 2 Linggong Rd., Dalian 116024, China

Supporting Information

ABSTRACT: Compared with traditional paper, water rewritable photonic crystal (PC) paper is an environmentally friendly and low resource-consuming material for information storage. Although, recently reported PC papers have high-quality structure color showing promising prospect, the paper size, that is within several centimeters, still limits turning it from potential to reality. Here, we present a new water rewritable PC film as large as the A4 size (210 × 300 mm^2) with a high-quality structure color. The material is prepared by thermal assisted self-assembly on the air−liquid interface. To fix such a large-area self-assembled PC film, we partially deform and coalesce the self-assembled nanoparticles, which have low glass transition temperature. This process causes the film to be transparent and structural colorless but still keeps the inner 3D-ordered structure. Then, utilizing the hydrophilic nature of the assembled block, the film can be switched to a structural color state by touching water. Diverse brilliant structural colors appear with different assembled particle (poly(butyl methacrylate-*co*-methylmethacrylate-*co*-butyl acrylate-*co*-diacetone acrylamide) named as PBMBD) sizes. The transparency−structural color transition can be performed multiple times reversibly in all or specific regions of the film. It provides a new solution for future applications of rewriteable PC paper.

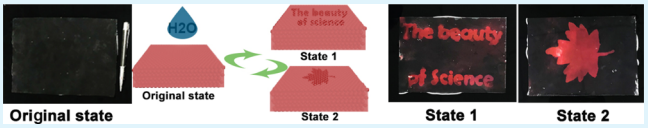

KEYWORDS: *large-area, photonic crystal film, water rewritable, structural color, thermal assisted air−liquid interface self assembly*

INTRODUCTION

The heavy use of traditional paper and ink causes a waste of resources and environmental pollution.[1] To alleviate this problem, rewritable paper with water "ink" has been proposed by many researchers. For example, Zhang et al. treated the surface of a paper with some specially designed dyes to make possible rewriting with water by changing the configuration and structure of the dyes.[2−4] Indeed, the dye-based paper exhibits pretty rewritable characteristics (excellent color uniformity, fast coloration, and purity). However, the application of dyes may cause other well-known problems of fading and emission of pollution.[5,6]

Different from traditional dyes, photonic crystal (PC) can produce bright and pollution-free structural color through diffracting or reflecting light waves selectively in its intrinsic periodic nanostructure.[7−12] Also, the color does not fade with periodic structure retention.[13−15] Hence, it evokes a lot of interest as a possible alternative to rewriteable papers replacing the type of dyes.[16−20] As a representative work, Ge et al. have developed a PCs paper/ink system. They used a poly(ethylene glycol)diacrylate-encapsulated Fe_3O_4@SiO_2 photonic structure as the paper and water as the ink.[21,22] In another work, a similar structure was built by embedding polystyrene (PS) colloidal crystal in chitosan hydrogel.[23] Once exposed to water, these materials experienced swelling, changed the parameters of the photonic structure, red-shifted the diffraction, and finally, created a color contrast with the unswollen part. These high-quality intrinsic periodic structures within several centimeters of size were prepared by the common assembly method, including magnetically or thermally induced self-assembly. Limited to inevitable cracking and polycrystallization, which degrade the optical properties of PC, common assembly methods generally face drawbacks in preparing large-scale PCs.[24,25]

For large-scale manufacturing of photonic structures, a high-quality, industrial processing method including pressing, extrusion, and rolling has been employed to arrange the core/shell polymer nanoparticles into an ordered structure for generating large-scale 3D polymer PCs.[25−29] These large-scale PCs have achieved great success in satisfying displaying, sensing, and patterning.[30−32] Besides the industrial processing method, some self-assembly methods have also been developed, such as inkjet printing technology[33,34] and spray coating[35] and bar coating techniques.[36−39] These methods are struggling against the "coffee ring" effect, which leads to limited pattern resolution and low color saturation.[36] The "coffee ring" effect is produced by the contact angle of the assembled liquid droplet in a hard substrate−liquid−air interface.[40−42] As an alternative to a hard substrate, an air−liquid interface can be used as a soft substrate to construct 3D PCs such as silica or polystyrene photonic structures without the "coffee ring" effect.[43,44] Large-area diffractive structure colors appearing on the interface indicates the formation of high-quality PC structure. However, to obtain the paper-like films, the difficulty is in transferring and fixing the floating 3D

Received: April 13, 2019
Accepted: June 5, 2019
Published: June 5, 2019

Downloaded via NOTTINGHAM TRENT UNIV on August 2, 2019 at 01:11:53 (UTC).
See https://pubs.acs.org/sharingguidelines for options on how to legitimately share published articles.

© 2019 American Chemical Society

DOI: 10.1021/acsami.9b06470
ACS Appl. Mater. Interfaces 2019, 11, 22777−22785

PC on the air−liquid interface, while holding its invariable and high-quality structure.

Herein, we propose a method to get rewritable freestanding PCs film with large-area and high-quality using the thermal assisted air−liquid interface self-assembly. As a key to our approach, the assembled block has a low glass transition temperature (T_g) and hydrophilicity. After self-assembly into a high-quality periodic structure on the air−liquid interface at a temperature slightly above T_g, the assembled particles undergo "partial deformation−coalescence" to form a fixed film and maintain an internal periodic structure. It also causes the film to lose structure color, accompanied by the boundary fusion of assembly particles. Then, we can switch the film to the structural color state by touching water based on its internal periodic structure and the hydrophilicity of the assembled block. The whole process can be summarized by Scheme 1. In

Scheme 1. Schematic Illustration of the Fabrication Process of the Large Area and Water Rewritable PBMBD PC Film and Corresponding Display of Structural Color with Water Touching

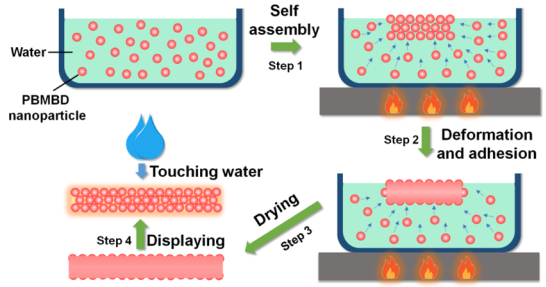

this work, we select poly(butyl methacrylate-*co*-methylmethacrylate-*co*-butyl acrylate-*co*-diacetone acrylamide) (PBMBD) nanoparticles as the assembled block to verify the feasibility of this idea and to test the relevant properties of the obtained material.

EXPERIMENTAL SECTION

Materials. The monomers of butyl methacrylate (BMA), methyl methacrylate (MMA), and butyl acrylate (BA) were all purchased from Tianjin Guangfu Chemical Co., Ltd. (Tianjin, China). Diacetone acrylamide (DAAM) was provided by Aladdin Chemistry Co., Ltd. (Shanghai, China). Sodium dodecyl sulfate (SDS), sodium bicarbonate, potassium persulfate (KPS) were purchased from Beijing Chemical Co., Ltd. (Beijing, China). The inhibitors were removed from the monomers by washing three times with aqueous NaOH (5 wt %), followed by washing six times with deionized water. Other reagents were used directly as received without further purification.

Synthesis of PBMBD Nanoparticles. As a typical example, the monodisperse negative-charged copolymer of P(BMA-MMA-BA-DAAM) particles with a T_g = 27 °C, named as PBMBD nanospheres, were prepared by emulsion polymerization. In brief, 120−240 mg of SDS and 1.62 g of $NaHCO_3$ were premixed with 1000 mL of deionized water for 20 min in a 2000 mL four-necked flask. Then, 72 mL of BMA, 54 mL of MMA, and 54 mL of BA monomer and 27 g of DAAM were added and stirred for another 20 min, followed by addition of 1.08 g of KPS. The whole mixing solution was deoxygenated by bubbling nitrogen gas. Then, the reaction was carried out under vigorous magnetic stirring at 70 °C for 5 h. Finally, the PBMBD particle size was controlled through the dosage of SDS. PBMBD nanoparticles with different T_g were synthesized by tuning ratio of three kinds of monomers corresponding to BMA, MMA, and BA, which showed in Table S1.

Synthesis of PBMB Nanoparticles. The monodisperse negative copolymer of P(BMA-MMA-BA) nanoparticles named as PBMB without the polymerizing DAAM monomer was prepared following similar procedures as described above.

Large-Scale Preparation of PBMBD PC Films. A thermal assisted air−liquid interface assembly was developed for preparing the large-area and water rewritable PC films. Typically, different concentrations of PBMBD water dispersion were placed in a glass dish with a size of 220 × 310 mm^2. The dish was heated at a different temperature from 40 to 120 °C on the heating plate with an open environment. Then, continuous and free-standing PBMBD PC films gradually formed at the air−liquid interface. The film was pulled out of the interface and dried at the glass substrate at 30−120 °C. Finally, a transparent free-standing PBMB PC film with a large area was prepared. The transparent films will display brilliant structural color once soaking or wetted with water.

Characterizations. The zeta potentials, particle size distribution index, and diameter (D) of PBMBD nanoparticles were measured by using a Zetasizer Nano Series Nano-ZS90 (Malvern, UK) at a wavelength of 633 nm. The morphologies of the monodisperse PBMBD nanoparticles and PBMBD PC films were investigated using FEI Nova NanoSEM 450 with 10 kV accelerating voltage. A Hitachi U-4100 spectrophotometer was used for the reflection and transmittance spectra of the PC films. The in situ optical reflection spectra

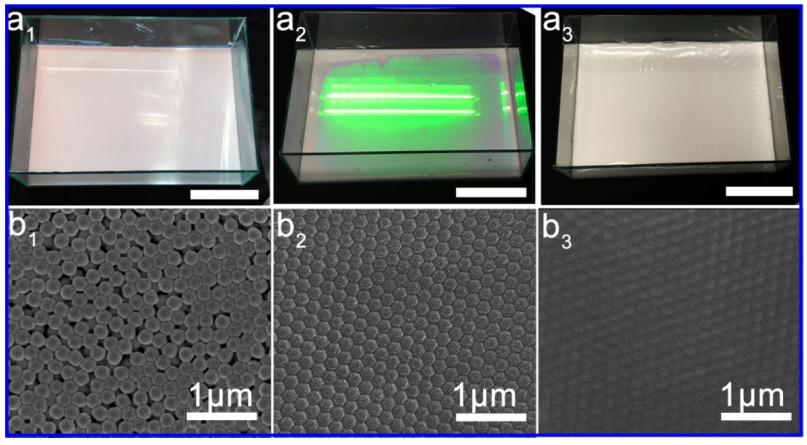

Figure 1. (a_1−a_3) Digital photographs corresponding to the three stages in the fabrication process of the transparent PC film: (a_1) 15 wt % PBMBD water dispersion; (a_2) floating iridescent PC film on the air−liquid interface; and (a_3) solid translucent PC films floating on the interface; (b_1−b_3) SEM image corresponding to the PBMBD PC films in different stages of a_1−a_3, respectively. The scale bars in (a_1−a_3) are 10 cm.

DOI: 10.1021/acsami.9b06470
ACS Appl. Mater. Interfaces 2019, 11, 22777−22785

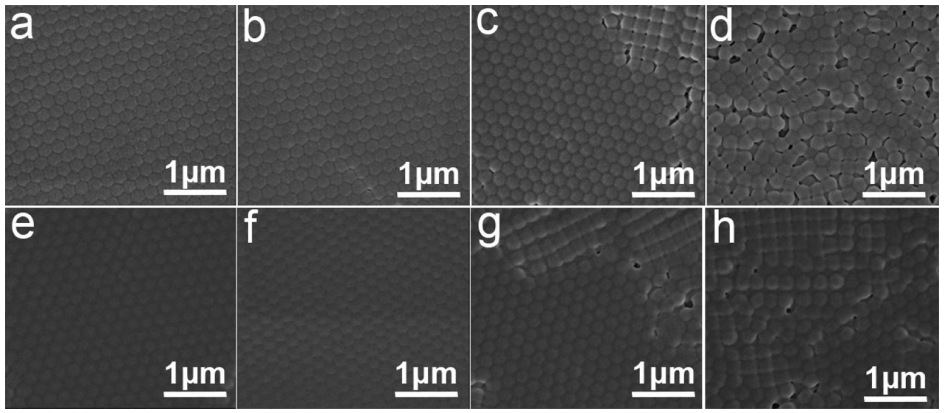

Figure 2. (a–d) SEM images of assembled PBMBD particles at the air–liquid interface with different evaporating temperatures. (a) 40; (b) 60; (c) 90; (d) 120 °C. (e–h) SEM images of the PBMBD PC films at the air–liquid interface after partial deformation–coalescence process corresponding to different evaporating temperatures (a–d), respectively.

were also obtained using a fiber optic spectrometer PG2000-Pro with a tungsten halogen light source. Optical photographs of the films were taken by using a Nikon digital camera. Differential scanning calorimetry (DSC) was carried out in a nitrogen atmosphere by using an American TA Instruments 910S DSC thermal analyzer from −20 to 200 °C at a heating rate of 5 °C/min. FT-IR spectra were recorded on a JASCO 430 spectrometer. The contact angles were investigated by a contact angle measuring instrument (JC2000C1). The refractive indexes of the PBMBD nanoparticles were determined by an M-2000 DI spectroscopic ellipsometer. The mechanical property, including tensile model, was measured by Precise PT-305 at 1 mm/min.

RESULTS AND DISCUSSIONS

Preparation and Optical Properties of the Large Area and Water Rewritable PBMBD PC Film. As shown in Figure 1, a self-assembly and subsequently partial deformation–coalescence process occurred on the air–liquid interface, which illustrated the feasibility of the design. In detail, PBMBD nanoparticles with T_g = 27 °C as a typical example, would undergo three typical stages to form a freestanding PCs film with a large area and high quality on the air–liquid interface (Figure 1a_1–a_3). These three stages were shown as follows: (1) heating a 15 wt % PBMBD water dispersion placed in an open glass vessel (a size of 220 × 310 mm^2) at an evaporating temperature slightly above T_g (Figure 1a_1). Because uniform sizes of the PBMBD nanoparticles facilitated the assembly of ordered arrays with highly quality. (Figure 1b_1), a close-packed layer of PBMBD particles were assembled at the air–liquid interface via thermal assisted evaporating driving force (Figure 1b_2).[36] (2) High-reflectance and brilliant iridescent film floating on the air–liquid interface illustrated the formation of ordered PBMBD arrays (Figure 1a_2). As the heating went on, the interstices between the PBMBD nanoparticles would shrink due to deformation against one another between soft PBMBD particles above their T_g. (3) As the interstices close off with deformation (Figure 1b_3), the brilliant iridescent color disappeared, and a translucent film was obtained with lacking refractive index contrast (Figure 1a_3).

The progress of self-assembly on the air–liquid interface was controlled by the heating-assisted temperature, namely, evaporating temperature, which directly determined the quality of the ordering photonic arrays. Figure 2a,b shows that low evaporating temperature was suitable for obtaining ordered fcc PC. Once the temperature rose higher than 90 °C, mixed photonic arrays and even disordered arrays occurred (Figure 2c,d). This phenomenon originated from too strong driving force to self-assemble into the ordered PC with a temperature higher than 90 °C. With mere consideration of self-assembly, the low evaporating temperature was more favorable to assemble into ordered photonic arrays. On the other hand, the low enough evaporating temperature (25 °C), that is even lower than T_g = 27 °C, of PBMBD particles could not fix the floating ordered photonic arrays into continuous and free-standing photonic arrays by providing partial deformation–coalescence (Figure S1a,b). Thus, the evaporating temperature higher than T_g (27 °C) was necessary to further shrink the interstices between the PBMBD nanoparticles for fixing and forming continuous and freestanding photonic arrays (Figure 2e–h). To bring about self-assembly into ordered photonic arrays and a subsequent partial deformation–coalescence process to fix an ordered structure, nanoparticles with low T_g (<60 °C) as the building blocks and an evaporating temperature slightly higher than T_g were the two critical elements for guaranteeing feasibility of the design.

After being peeled off from the air–liquid interface and dried at a controlled temperature, a totally colorless and transparent PBMBD PC film was obtained via further coalescence of these PBMBD particles across the particle boundaries and entangling. The thickness of the final PC films varied from 69.5 to 102.5 μm with increasing concentration of the PBMBD water dispersion shown in Table S2. As the thickness of PC films increased, the transparency was hardly distinguished directly by a digital photograph (Figure S2a). For further confirming this result, a transmittance spectra of the PBMBD 3D PC films with different thicknesses were obtained and are shown in Figure S2b. It was clearly seen that there is nearly no distinction in transparency induced by the thickness of the PC film. The thickness not specially mentioned was 102.5 μm in the following representation, which is close to the thickness of A4 paper (104 μm). The Figure 3a shows that the obtained PBMBD 3D PC film was as large as an A4 paper (210 mm × 300 mm) but also high transparency for displaying clear pattern under it. The transparency spectra in Figure 3b further illustrated higher than 87.5% transparent property for the PBMBD 3D PC films. Besides, the films could be rolled into a cylinder, which demonstrated their excellent flexibility (Figure 3c). This flexibility was endowed by the soft polymer property of PBMBD with a low T_g = 27 °C, which is close to room

DOI: 10.1021/acsami.9b06470
ACS Appl. Mater. Interfaces 2019, 11, 22777–22785

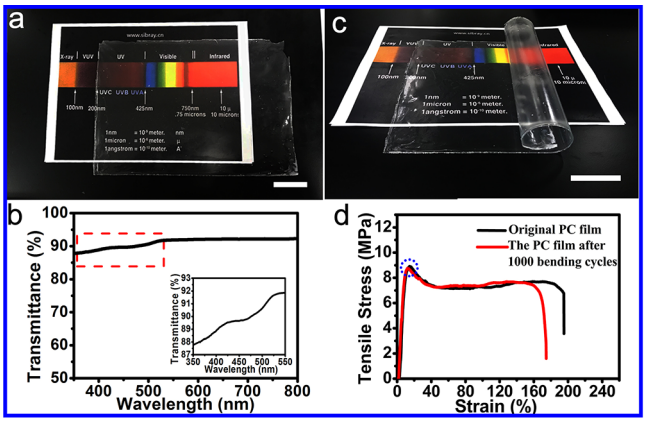

Figure 3. (a) Transparent and colorless PBMBD 3D PC films as large as A4 papers. (b) Transmittance spectra of the PBMBD 3D PC films. (c) Bending property of the PBMBD 3D PC films. (d) Representative tensile stress−strain curves of the original PBMBD PC film (black line) and the PBMBD PC film after conducting 1000 bending circles (red line). The blue circle region represents the yield point of the PC film. The scale bars in (a,c) are 5 cm.

temperature. The mechanical strength test was also conducted for the PC films, and the results are shown in Figure 3d. The PBMBD PC film could resist yield strength as high as 8.9 MPa, which demonstrated excellent resisting tensile capacity. In addition, a yield point existed in the blue circle region of the stress−strain curve before cold-drawing, indicating the tough ductile property of the PC film. For further demonstration of the change in the toughness property after experiencing 1000 bending cycles, we conducted a bending measurement by a self-made bending equipment (Movie S1) with bending 1000 times and then, carrying out the tensile stress−strain measurement. The result showed no dramatic change in the position of the yield point and mechanical property (Figure 3d). Thus, the toughness property of the PC film was satisfactory for acting as a PC paper.

An interesting phenomenon appears once the film meets water. A brilliant structural color emerges instead of the originally colorless and transparent feature within 10 s (Movie S2). Indeed, the PBMBD PC film as large as an A4 paper displays uniform structural color rapidly after water wetting. Moreover, the color of the film could be tuned by varying the PBMBD nanoparticle size, by referring to the Bragg diffraction formula of 3D PC. With tuning the PBMBD particle sizes from 287, 224, to 195 nm (Figure S3), the water-wetted PC films display three different kinds of structural colors, namely red, green, and blue, respectively, in the 10° observing angle (Figure 4a−c). The reflection spectra of these three water-wetted PC films were measured by varying the angle of incidence from 10° to 50°. It could be clearly seen that the reflection spectra with a 10° incidence angle is in accordance with the displaying structural color. Also, the dramatic blue shift in the reflection peak position occurs with increasing of the viewing angle from 10° to 50°, which is a typical feature of the 3D PC (Figure 4d−f). The calculated wavelength (λ_{max}) of the stop-band could be estimated by the Bragg's law: $\lambda_{max} = (8/3)^{1/2}D(n_{eff}^2 - \sin^2\theta)^{1/2}$, where λ_{max} is the wavelength at the peak position, D is the diameter of PBMBD nanoparticles, and θ is the angle between the incident light and the reflective surface. The n_{eff} is the effective refractive index, which can be expressed as $n_{eff}^2 = n_{PBMBD}^2\varphi_{PBMBD} + n_{H_2O}^2\varphi_{H_2O}$. n_{PBMBD} is 1.43 in the visible light region (400−800 nm) (Figure S4), n_{H_2O} is 1.33. φ_{PBMBD} and φ_{H_2O} are the volume fractions and are 0.74 and 0.26, respectively, for an ideal fcc structure assembled by PBMBD nanoparticles, and water occupying their interstices. Thus, Table S3 shows the calculated and measured λ_{max} for

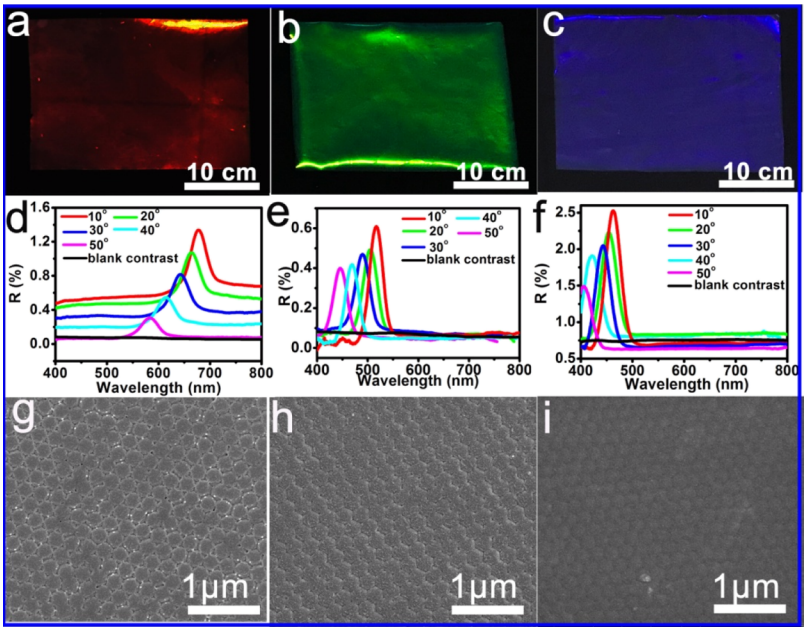

Figure 4. Digital photographs of the PBMBD PC films assembled from particle sizes of 287, 224, and 195 nm, respectively, displaying red (a); green (b); and blue (c) with water wetting. (d−f) Corresponding reflection spectra of the three PBMBD PC films in different viewing angles with varying PBMBD nanoparticle sizes of 287 (d), 224 (e), and 195 nm (f), respectively (the black line represents PC films without water wetting). SEM images of the water-wetted PBMBD PC films after being freeze-dried, corresponding to a different diameter of PBMBD. (g) 287; (h) 224; (i) 195 nm.

DOI: 10.1021/acsami.9b06470
ACS Appl. Mater. Interfaces 2019, 11, 22777−22785

three kinds of water-wetted PBMBD PC films with different PBMBD particle sizes. It is noteworthy that the calculated λ_{max} from the Bragg's equation has little difference with the measured values in reflection spectra, which can be explained by rebuilding the 3D PC with the participation of water.

In addition, the top view and cross-sectional scanning electron microscopy (SEM) images of the water-wetted PC film (being freeze-dried) in Figures 4g–i and S5, indeed, demonstrate the existence of a 3D highly ordered nanostructure after water wetting. Even the ordered structure of the PBMBD PC films could be kept with length scales as large as nearly 15 μm (Figure S6).

The stability results of water-wetted PC films were of great importance for characterizing the water writing property of the PC films. The PC film displayed increasing reflectance peak height with primary interaction with water with respect to the interacting time needed in the thickness of PC structure (Figure 5a).[24] After exceeding 6 s, the reflectance peak height

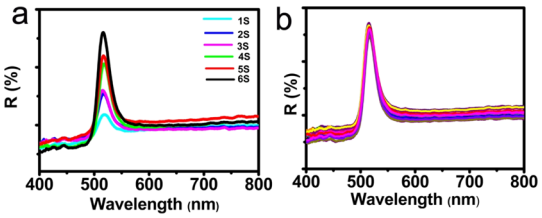

Figure 5. Specific reflectance spectra contrast of the water-wetted 224 nm PBMBD PC films with a change of time: (a) average one time per second. (b) Average one time per 30 min in the whole 12 h.

nearly stayed invariable for 12 h, which implied excellent stability of structural color for PC films in an aqueous solution (Figure 5b). Furthermore, we also investigated the possible responses of these PC films to other polar or nonpolar fluids with different refractive indexes. The result is displayed in Figure S7 showing water as the perfect tool to use as ink to write patterns on the rewriteable PC films.

The brilliant structural color of the water-wetted PC films could be reverted to transparent and colorless by drying the water at room temperature, and the dried PC films would display structural color after water wetting again. The result is shown in Figure 6a where brilliant red handwriting was displayed in the transparent PBMBD PC film when using a water pen to write on the film. The pattern of handwriting could exist on the paper until the water had been evaporated at room temperature. Also, a transparent PC film without a writing trace (Figure 6b) could be employed again by water writing another pattern just like a maple leaf in Figure 6c. It was of great importance that the film had good stability in reversible water-wetted structural color with basically invariable position and height of the reflection peak over 10 cycles (Figure 6c,d). In a word, this kind of large-area PBMBD PC film had excellent water rewritable property.

Properties and Mechanism of Water Writable Structural Color for PBMBD PC Films. The properties of water writable structural color including uniformity/purity, displaying rate, and brightness were determined by the thermal assisted temperature and thickness. In detail, the uniform/purity structural color of the water-wetted PBMBD PC film was dominated by evaporating temperature on the air–liquid interface. Considering that the evaporative flux across the air–liquid interface was proportional to the evaporating temperature, high evaporative flux would bring such a strong capillary flow for self-assembly that there would not be enough time for a completely ordered fcc nanostructure to assemble.[36] As pointed in Figure 7c–f, the morphology of the obtained PBMBD PC films at different evaporating temperatures from 40 to 120 °C, which are above the T_g of PBMBD, can hardly be distinguished from the others because of a different degree of deformation and coalescence between the individual PBMBD particles (Figure 7b). However, the ordered structures of fcc arrays of the water-wetted PBMBD PC film was disturbed by other arrays and even became disordered as the evaporating temperature increased gradually from 40 to 120 °C. This ordered–disordered transition indeed brought impure structural color where the green structural color for the water wetting PC films gradually mixed with the yellow structural color (Figure 7a).

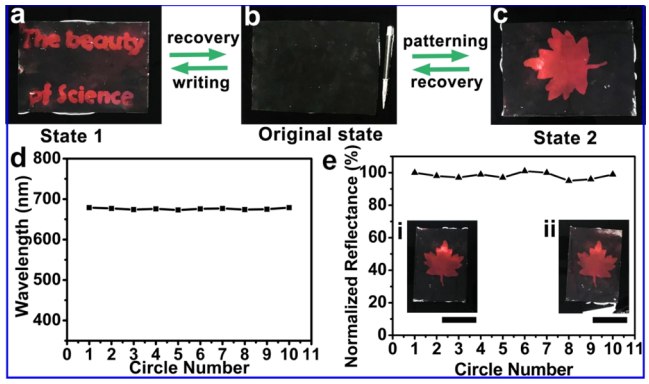

Figure 6. The process of the red PBMBD PC film for water writing and patterning 10 times repeatedly. (a) State 1: English phrase was written by a water pen. (b) Original state: a transparent and colorless PBMBD PC film. (c) State 2: the pattern of a maple leaf was left on the film by writing with water. (d) Diffraction wavelengths of the PBMBD PC film in 10 cycles by writing with water and erasing by water evaporation. (e) Height of reflectance peak of the PC film changes in 10 cycles by reversibly writing and evaporating water, digital photos of the colored films written with water in (i) first circle, (ii) the 10th circle. The scale bar is 10 cm.

For the water-wetted PC film, the discoloring rate and displaying brightness were determined by the drying temperature in the drying stage. The brightness could be evaluated definitely by the height of the reflectance peak. Thus, the reflectance peak height, the reacting time, and the drying temperature are drawn in Figure 8b. With increasing the drying temperature from 30 to 120 °C, there was a dramatic drop in the height of the reflecting peak of the water-wetted PC films, which indicated that higher temperature above the T_g (27 °C) would lead to more reduced brightness of the structural color (Figure 8a). Meanwhile, the PBMBD PC films obtained at low drying temperature only took less than 10 s to display green structural color after water wetting. Once the drying temperature was improved to 120 °C, the time needed to display the structural color increased by more than 20 times. As shown in Figure 8c–f, all PBMBD PC films had coalescence-led flattened arrays, which had similar morphology as that of the pure PBMBD polymer (Figure S8 pure polymer). With increasing the drying temperature from 30 to 80 °C, the fcc arrays became vague and regional, which indicated that the degree of deformation–coalescence had deepened (Figure 8g–i). Once the temperature increased to 120 °C, the PC films exhibited only single PBMBD particles occasionally without

DOI: 10.1021/acsami.9b06470
ACS Appl. Mater. Interfaces 2019, 11, 22777–22785

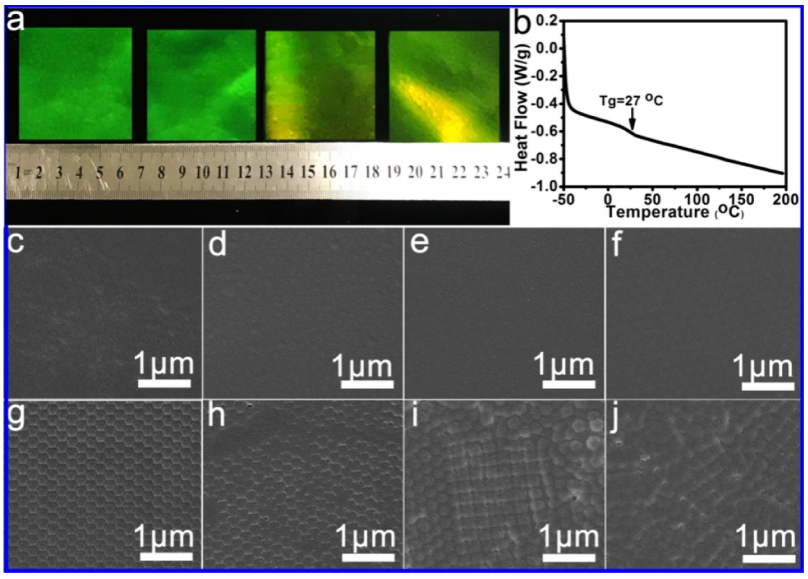

Figure 7. (a) From left to right: the images of structural colors for different PBMBD PC films after water wetting corresponding to formation at a different evaporating temperature of 40, 60, 90, and 120 °C, respectively. (b) DSC curve of the PBMBD PC films. (c–f) SEM images of the colorless PBMBD PC films with different evaporating temperatures. (c) 40; (d) 60; (e) 90; (f) 120 °C. (g–j) SEM images of the PBMBD PC films which maintain the water wetting structure by freeze-drying, corresponding to different evaporating temperatures (c–f), respectively.

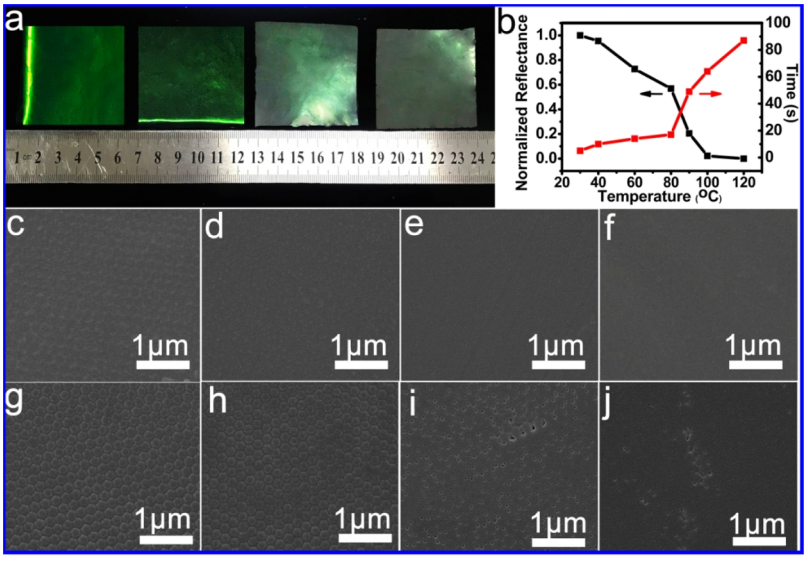

Figure 8. (a) From left to right: the images of different PBMBD PC films with varying structural color after water wetting, corresponding to formation at different drying temperatures of 30, 60, 90, and 120 °C, respectively. (b) Changes in the reflectance height and displaying time from transparent and colorless to brilliant structural color after water wetting as a function of the drying temperature for the PBMBD PC films. (c–f) SEM images of the colorless and transparent PBMBD PC films with different drying temperatures of (c) 30, (d) 60, (e) 80, (f) 120 °C, respectively. (g–j) SEM images of the water-wetted PBMBD PC films after being freeze-dried corresponding to (c–f), respectively.

ordered PBMBD arrays after water wetting, which indicated complete coalescence of inner PBMBD particles (Figure 8j). In a word, the deepened deformation–coalescence led to delay in the displaying rate and decreased brightness. The PBMBD PC film with different T_g (Figure S9) was obtained at the optimized thermal assisted temperature, which is shown in Table S4. It illustrated the feasibility of thermal assisted air–liquid interface self-assembly for preparing PC films with different T_g.

Besides, as the thickness of the PC film increased with varying concentrations of the PBMBD water dispersion from 1 to 15%, the height of the reflectance peak slightly increased, which meant that the thickness of the PC film affected the brightness of the structural color (Figure S10). This was determined by percolation of water in the interstices of the PBMBD particles to produce a refractive contrast for rebuilding the structural color.

Inspired by the Gu et al. article about a hydrophobic continuous elastic film with water-responsive structural color,[45,46] we inferred similar discoloring mechanism to exist in this work where the confluent spheres turned back to the separated soft spheres with water wetting and rebuilt the structural color under the refractive contrast of separated soft spheres and water. In addition, the SEM images in Figures 7c–j and 8c–j showed that the separate spheres appeared again, once the confluent and continuous spheres met water.

DOI: 10.1021/acsami.9b06470
ACS Appl. Mater. Interfaces 2019, 11, 22777–22785

Considering that the hydrophobic film was not conducive to water spreading on its surface, slightly hydrophilic PBMBD nanoparticles were obtained via polymerizing the hydrophilic DAAM monomer with the other three hydrophobic monomers of BMA, MMA, and BA. As a contrast, totally hydrophobic poly(butyl methacrylate-*co*-methyl methacrylate-*co*-butyl acrylate) (PBMB) nanoparticles were also prepared. The IR spectra and wetting measurements indeed demonstrate that the hydrophilic property appeared with adding the DAAM units (Figures S11 and S12). The PBMBD PC film exhibited water-responsive discoloring within 10 s, which was much faster than the water-responsive rate of the PBMB PC film (Table S5), which proved that the hydrophilic property of PBMBD was a prerequisite for water-writable capacity.

CONCLUSIONS

A large-area and water rewritable PC film was prepared for the first time by thermal assisted air−liquid interface self-assembly. This kind of PBMBD PC films possessed high transparency and excellent flexibility under drying conditions. Once being water wetted, the obtained hydrophilic PBMBD PC film could transform rapidly from being transparent and colorless to showing corresponding brilliant structural color. The corresponding structural color was tuned by varying particle sizes of PBMBD particles. The structural colors were reversible and recyclable with or without water wetting. These excellent properties of the structural color including uniformity/purity, rapid discoloring rate, and displaying brightness were realized by carefully controlling thermal assisted temperature slightly above the T_g of PBMBD particles. This kind of large-area PC films using water writing or patterning are a potential candidate for replacing traditional one-time use papers.

ASSOCIATED CONTENT

Supporting Information

The Supporting Information is available free of charge on the ACS Publications website at DOI: 10.1021/acsami.9b06470.

PBMBD nanoparticles with different T_g obtained under different ratio of monomers with fixing DAAM; photographs of a floating iridescent PC film on the air−liquid interface at the evaporating temperature of 25 °C and a disturbed iridescent PC film on the air−liquid interface without being fixed into continuous and freestanding PC film; thickness of PBMBD PCs films under different concentrations of PBMBD water dispersion; photographs and transmittance spectra of PBMBD PC films with different thicknesses; SEM images of PBMBD nanoparticles with different diameters and size distribution diagrams of the PBMBD spheres; refractive index of PBMBD; measured diameters of PBMBD nanoparticles and calculated n_{eff}, calculated λ_{max}, and measured λ_{max} of their corresponding water wetted PC films; cross-sectional SEM image of the water wetted 224 nm PBMBD PCs film after being freeze-dried; SEM image of large-scale water wetted PBMBD PCs films with different particle sizes of PBMBD (after being freeze-dried); digital photograph of PBMBD PC films and PBMBD PC films after soaking in different solvents; SEM image of pure PBMBD polymer; DSC curve of the PBMBD PC films with different T_g; relationship between T_g of PBMBD PC film and optimized thermal assisted temperature including evaporating temperature and drying temperature; Fourier transform infrared spectra for PBMB and PBMBD polymers; wetting properties of the surface of the PBMB and PBMBD 3D PCs films; and transforming time from transparency and colorless to brilliant green structural color for two kinds of PCs films with different contact angle (PDF)

Bending measurement by self-made bending equipment after 1000 bending cycles (MP4)

Rapid transformation from originally colorless and transparent to brilliant structural color (MP4)

AUTHOR INFORMATION

Corresponding Author

*E-mail: zhangshf@dlut.edu.cn.

ORCID

Wenbin Niu: 0000-0001-5507-1592

Suli Wu: 0000-0002-3956-1855

Wei Ma: 0000-0003-2283-9563

Shufen Zhang: 0000-0003-3390-4199

Author Contributions

All authors have given approval to the final version of the manuscript.

Funding

This work is supported by the State Key Program of the National Natural Science Foundation of China (21536002), the Science Fund for Creative Research Groups of the National Natural Science Foundation of China (21421005), Ministry of Education (the Ministry of Education Innovation Team, IRT-13R06), and Dalian University of Technology (Dalian University of Technology Innovative Research Team, DUT2013TB07).

Notes

The authors declare no competing financial interest.

ABBREVIATIONS

PCs, photonic crystal

PBMBD, poly(butyl methacrylate-*co*-methylmethacrylate-*co*-butyl acrylate-*co*-diacetone acrylamide)

PBMB, poly(butyl methacrylate-*co*-methylmethacrylate-*co*-butyl acrylate)

REFERENCES

(1) Sarantis, H. Business Guide to Reducing Paper Usage, MSc Thesis, University of Montana, 2002, pp 1−63.

(2) Xi, G.; Sheng, L.; Du, J.; Zhang, J.; Li, M.; Wang, H.; Ma, Y.; Zhang, S. X. Water Assisted Biomimetic Synergistic Process and Its Application in Water-Jet Rewritable Paper. *Nat. Commun.* **2018**, *9*, 4819−4827.

(3) Singh, V. K.; Chitumalla, R. K.; Ravi, S. K.; Zhang, Y.; Xi, Y.; Sanjairaj, V.; Zhang, C.; Jang, J.; Tan, S. C. Inkjet-Printable Hydrochromic Paper for Encrypting Information and Anticounterfeiting. *ACS Appl. Mater. Interfaces* **2017**, *9*, 33071−33079.

(4) Sheng, L.; Li, M.; Zhu, S.; Li, H.; Xi, G.; Li, Y. G.; Wang, Y.; Li, Q.; Liang, S.; Zhong, K.; Zhang, S. X. Hydrochromic Molecular Switches for Water-Jet Rewritable Paper. *Nat. Commun.* **2014**, *5*, 3044.

(5) Wang, W.; Xie, N.; He, L.; Yin, Y. D. Photocatalytic Colour Switching of Redox Dyes for Ink-Free Light-Printable Rewritable Paper. *Nat. Commun.* **2014**, *5*, 5459.

(6) Xi, G.; Sheng, L.; Zhang, I.; Du, J.; Zhang, T.; Chen, Q.; Li, G.; Zhang, Y.; Song, Y.; Li, J.; Zhang, Y.-M.; Zhang, S. X.-A. Endowing Hydrochromism to Fluorans Via Bioinspired Alteration of Molecular

DOI: 10.1021/acsami.9b06470
ACS Appl. Mater. Interfaces 2019, 11, 22777−22785

Structures and Microenvironments and Expanding Their Potential for Rewritable Paper. *ACS Appl. Mater. Interfaces* **2017**, *9*, 38032−38041.
(7) Stein, A.; Wilson, B. E.; Rudisill, S. G. Design and Functionality of Colloidal-Crystal-Templated Materials-Chemical Applications of Inverse Opals. *Chem. Soc. Rev.* **2013**, *42*, 2763−2803.
(8) von Freymann, G.; Kitaev, V.; Lotsch, B. V.; Ozin, G. A. Bottom-up Assembly of Photonic Crystals. *Chem. Soc. Rev.* **2013**, *42*, 2528−2554.
(9) Cong, H.; Yu, B.; Tang, J.; Li, Z.; Liu, X. Current Status and Future Developments in Preparation and Application of Colloidal Crystals. *Chem. Soc. Rev.* **2013**, *42*, 7774−7800.
(10) Galisteo-López, J. F.; Ibisate, M.; Sapienza, R.; Froufe-Pérez, L. S.; Blanco, Á.; López, C. Self-Assembled Photonic Structures. *Adv. Mater.* **2011**, *23*, 30−69.
(11) Yu, S.-Z.; Niu, W.-B.; Wu, S.-L.; Ma, W.; Zhang, S.-F. Robust and Flexible Thermal-Plasticizing 3D Shaped Composite Films with Invariable and Brilliant Structural Color. *J. Mater. Chem. C* **2018**, *6*, 12814−12821.
(12) Schaffner, M.; England, G.; Kolle, M.; Aizenberg, J.; Vogel, N. Combining Bottom-up Self-Assembly with Top-Down Microfabrication to Create Hierarchical Inverse Opals with High Structural Order. *Small* **2015**, *11*, 4334−4340.
(13) Li, Q.; Zhang, Y.; Shi, L.; Qiu, H.; Zhang, S.; Qi, N.; Hu, J.; Yuan, W.; Zhang, X.; Zhang, K.-Q. Additive Mixing and Conformal Coating of Noniridescent Structural Colors with Robust Mechanical Properties Fabricated by Atomization Deposition. *ACS Nano* **2018**, *12*, 3095−3102.
(14) Wang, F.; Zhang, X.; Lin, Y.; Wang, L.; Zhu, J. Structural Coloration Pigments Based on Carbon Modified Zns@SiO2 Nanospheres with Low-Angle Dependence, High Color Saturation, and Enhanced Stability. *ACS Appl. Mater. Interfaces* **2016**, *8*, 5009−5016.
(15) Li, F.; Tang, B. T.; Wu, S. L.; Zhang, S. F. Facile Synthesis of Monodispersed Polysulfide Spheres for Building Structural Colors with High Color Visibility and Broad Viewing Angle. *Small* **2017**, *13*, 1602565.
(16) Kim, H.; Ge, J.; Kim, J.; Choi, S.-e.; Lee, H.; Lee, H.; Park, W.; Yin, Y.; Kwon, S.; Mitropoulos, A. N. Structural Colour Printing Using a Magnetically Tunable and Lithographically Fixable Photonic Crystal. *Nat. Photon.* **2009**, *3*, 534−540.
(17) Bai, L.; Xie, Z.; Wang, W.; Yuan, C.; Zhao, Y.; Mu, Z.; Zhong, Q.; Gu, Z. Bio-Inspired Vapor-Responsive Colloidal Photonic Crystal Patterns by Inkjet Printing. *ACS Nano* **2014**, *8*, 11094−11100.
(18) Ye, S.; Fu, Q.; Ge, J. Invisible Photonic Prints Shown by Deformation. *Adv. Funct. Mater.* **2014**, *24*, 6430−6438.
(19) Kang, H. S.; Lee, J.; Cho, S. M.; Park, T. H.; Kim, M. J.; Park, C.; Lee, S. W.; Kim, K. L.; Ryu, D. Y.; Huh, J.; Thomas, E. L.; Park, C. Printable and Rewritable Full Block Copolymer Structural Color. *Adv. Mater.* **2017**, *29*, 1700084−1700091.
(20) Wang, Y.; Aurelio, D.; Li, W.; Tseng, P.; Zheng, Z.; Li, M.; Kaplan, D. L.; Liscidini, M.; Omenetto, F. G. Modulation of Multiscale 3D Lattices through Conformational Control: Painting Silk Inverse Opals with Water and Light. *Adv. Mater.* **2017**, *29*, 1702769.
(21) Ge, J.; Goebl, J.; He, L.; Lu, Z.; Yin, Y. Rewritable Photonic Paper with Hygroscopic Salt Solution as Ink. *Adv. Mater.* **2009**, *21*, 4259−4264.
(22) Xuan, R.; Ge, J. Invisible Photonic Prints Shown by Water. *J. Mater. Chem.* **2012**, *22*, 367−372.
(23) Du, X.; Li, T.; Li, L.; Zhang, Z.; Wu, T. Water as a colorful ink: transparent, rewritable photonic coatings based on colloidal crystals embedded in chitosan hydrogel. *J. Mater. Chem. C* **2015**, *3*, 3542−3546.
(24) Shen, Z.; Shi, L.; You, B.; Wu, L.; Zhao, D. Large-Scale Fabrication of Three-Dimensional Ordered Polymer Films with Strong Structure Colors and Robust Mechanical Properties. *J. Mater. Chem.* **2012**, *22*, 8069−8075.
(25) Pursiainen, O. L. J.; Baumberg, J. J.; Winkler, H.; Viel, B.; Spahn, P.; Ruhl, T. Shear-Induced Organization in Flexible Polymer Opals. *Adv. Mater.* **2008**, *20*, 1484−1487.
(26) Snoswell, D. R. E.; Kontogeorgos, A.; Baumberg, J. J.; Lord, T. D.; Mackley, M. R.; Spahn, P.; Hellmann, G. P. Shear Ordering in Polymer Photonic Crystals. *Phys. Rev. E: Stat., Nonlinear, Soft Matter Phys.* **2010**, *81*, 020401.
(27) Finlayson, C. E.; Spahn, P.; Snoswell, D. R. E.; Yates, G.; Kontogeorgos, A.; Haines, A. I.; Hellmann, G. P.; Baumberg, J. J. 3D Bulk Ordering in Macroscopic Solid Opaline Films by Edge-Induced Rotational Shearing. *Adv. Mater.* **2011**, *23*, 1540−1544.
(28) Zhao, Q.; Finlayson, C. E.; Snoswell, D. R.; Haines, A.; Schafer, C.; Spahn, P.; Hellmann, G. P.; Petukhov, A. V.; Herrmann, L.; Burdet, P.; Midgley, P. A.; Butler, S.; Mackley, M.; Guo, Q.; Baumberg, J. J. Large-Scale Ordering of Nanoparticles Using Viscoelastic Shear Processing. *Nat. Commun.* **2016**, *7*, 11661−11670.
(29) Finlayson, C. E.; Baumberg, J. J. Generating Bulk-Scale Ordered Optical Materials Using Shear-Assembly in Viscoelastic Media. *Materials* **2017**, *10*, 688−702.
(30) Gallei, M. Functional Polymer Opals and Porous Materials by Shear-Induced Assembly of Tailor-Made Particles. *Macromol. Rapid Commun.* **2018**, *39*, 1700648−1700664.
(31) Schäfer, C. G.; Winter, T.; Heidt, S.; Dietz, C.; Baumberg, J. J.; Gallei, M. Smart polymer inverse-opal photonic crystal films by melt-shear organization for hybrid core-shell architectures. *J. Mater. Chem. C* **2015**, *3*, 2204−2214.
(32) Schäfer, C. G.; Gallei, M.; Zahn, J. T.; Engelhardt, J.; Hellmann, G. P.; Rehahn, M. Reversible Light-, Thermo-, and Mechano-Responsive Elastomeric Polymer Opal Films. *Chem. Mater.* **2013**, *25*, 2309−2318.
(33) Bao, B.; Sun, J.; Gao, M.; Zhang, X.; Jiang, L.; Song, Y. Patterning Liquids on Inkjet-Imprinted Surfaces with Highly Adhesive Superhydrophobicity. *Nanoscale* **2016**, *8*, 9556−9562.
(34) Huang, Y.; Li, F.; Qin, M.; Jiang, L.; Song, Y. A Multi-Stopband Photonic-Crystal Microchip for High-Performance Metal-Ion Recognition Based on Fluorescent Detection. *Angew. Chem., Int. Ed.* **2013**, *52*, 7296−7299.
(35) Ge, D.; Lee, E.; Yang, L.; Cho, Y.; Li, M.; Gianola, D. S.; Yang, S. A Robust Smart Window: Reversibly Switching from High Transparency to Angle-Independent Structural Color Display. *Adv. Mater.* **2015**, *27*, 2489−2495.
(36) Zhang, J.; Zhu, Z.; Yu, Z.; Ling, L.; Wang, C.-F.; Chen, S. Large-Scale Colloidal Films with Robust Structural Colors. *Mater. Horiz.* **2019**, *6*, 90−96.
(37) Zhang, J.; Yang, S.; Tian, Y.; Wang, C.-F.; Chen, S. Dual Photonic-Bandgap Optical Films Towards the Generation of Photonic Crystal-Derived 2-Dimensional Chemical Codes. *Chem. Commun.* **2015**, *51*, 10528−10531.
(38) Liu, K.; Tian, Y.; Li, Q.; Du, X.-Y.; Zhang, J.; Wang, C.-F.; Chen, S. Microfluidic Printing Directing Photonic Crystal Bead 2D Code Patterns. *J. Mater. Chem. C* **2018**, *6*, 2336−2341.
(39) Peng, G.; Zhu, Z.; Tian, Y.; Tong, Y.-l.; Cui, T.-T.; Wang, C.-F.; Chen, S. Dendrimer-Induced Colloids Towards Robust Fluorescent Photonic Crystal Films and High Performance Wleds. *J. Mater. Chem. C* **2018**, *6*, 8187−8193.
(40) Deegan, R. D.; Bakajin, O.; Dupont, T. F.; Huber, G.; Nagel, S. R.; Witten, T. A. Capillary Flow as the Cause of Ring Stains from Dried Liquid Drops. *Nature* **1997**, *389*, 827−829.
(41) Xie, Z.; Li, L.; Liu, P.; Zheng, F.; Guo, L.; Zhao, Y.; Jin, L.; Li, T.; Gu, Z. Self-Assembled Coffee-Ring Colloidal Crystals for Structurally Colored Contact Lenses. *Small* **2015**, *11*, 926−930.
(42) Shastry, T. A.; Seo, J.-W. T.; Lopez, J. J.; Arnold, H. N.; Kelter, J. Z.; Sangwan, V. K.; Lauhon, L. J.; Marks, T. J.; Hersam, M. C. Large-Area, Electronically Monodisperse, Aligned Single-Walled Carbon Nanotube Thin Films Fabricated by Evaporation-Driven Self-Assembly. *Small* **2013**, *9*, 45−51.
(43) Im, S. H.; Lim, Y. T.; Suh, D. J.; Park, O. O. Three-Dimensional Self-Assembly of Colloids at a Water-Air Interface: A Novel Technique for the Fabrication of Photonic Bandgap Crystals. *Adv. Mater.* **2002**, *14*, 1367−1369.

DOI: 10.1021/acsami.9b06470
ACS Appl. Mater. Interfaces 2019, 11, 22777−22785

(44) Li, W.; Fu, T.; He, S. Preparation of free-standing silica 3D colloidal crystal film at water-air interface. *Mater. Sci. Eng., A* **2006**, *441*, 239−244.
(45) Sun, C.; Yao, Y.; Gu, Z. Fabrication of elastic colloidal crystal films from pure soft spheres. *Colloids Surf., A* **2012**, *402*, 102−107.
(46) Sun, C.; Yao, J.; Yao, Y. Fabrication of Elastic Colloidal Crystal Films from P(MMA-BA) Soft Spheres. *Mater. Rev.* **2013**, *27*, 84−89.

DOI: 10.1021/acsami.9b06470
ACS Appl. Mater. Interfaces 2019, 11, 22777−22785